Indian Journal of Pure & Applied Physics
Vol. 61, September 2023, pp. 762-764
DOI: 10.56042/ijpap.v61i9.3494

Synthetization and Characterization of Mg-doped SnSe with Mg Substitution at the Sn Site by High Energy Ball Milling Technique

Mukesh Kumar Bairwa[a], R Gowrishankar[b], Anjali Saini[a] & S Neeleshwar[a*]

[a]University School of Basic and Applied Sciences, Guru Gobind Singh Indraprastha University, Delhi 110 078, India

[b]Department of Physics, Sri Sathya Sai Institute of Higher Learning, Prasanthinilayam, A.P 515 134, India

Received 9 July 2023; accepted 11 August 2023

Tin selenide (SnSe) is a semiconductor with an orthorhombic crystal structure having an indirect and direct band gap of 0.9 eV and 1.3 eV respectively. The SnSe and Mg-doped SnSe was synthesized by high energy ball milling technique at 300 RPM for 22 hrs. The formation of pure orthorhombic phases of SnSe and Mg-doped SnSe were confirmed by X-ray diffraction (XRD). From the XRD pattern, the crystalline size was estimated which lies below ~10 nm. The morphology of particle size distribution was carried out by scanning electron microscopy (SEM).

Keywords: Phase purification; Ball milling; SnSe; Doping

1 Introduction

SnSe is a well-known p-type semiconductor which has many applications in areas such as thermoelectric[1], photovoltaics[2], solar cells[3], electronics[4], optics[5], infrared optoelectronic devices[6], phase change memory alloys[7] and flexible systems[8]. SnSe is a layered orthorhombic crystal structure, where the atoms are connected with strong hetero-polar bonds and form a zigzag chain like structure[9,10], as shown in Fig. 1. The adjacent layers are bound by van der Waals forces and long-range electrostatic attraction, that easily break on applying shear force[9,11]. Generally, SnSe undergoes a structural phase transition from its initial *Pnma* (orthorhombic) structure to a *Cmcm* (monoclinic) structure above 750 K[12]. During this transition, the c-axis of the crystal lattice shortens, *i.e.*, the c-axis closely resemble to b-axis. This structural change occurs due to the compression of the intrinsically deformable, zig-zag "accordion-like" layer geometry[13].

SnSe has multi domain applications, and therefore it is significant to synthesize SnSe by cost effective, environmentally friendly, non-toxic and scalable processes. To date, many experimental and theoretical investigations have been carried out to understand the transport mechanism of SnSe through compositional optimization of carrier concentration by doping (Li[14], Na[15], Ag[16], Cu[17], Ge[18]) and co-doping (Na+X, X=K[19], Ag[20] *etc.*).

So far, SnSe has been synthesized by ball milling, hydrothermal, refluxing method, melt-growth and Bridgeman technique[21,22,23]. All these techniques have their own advantages and disadvantages. Among them, high energy ball milling is a cost effective, non-toxic and scalable technique. In this study, SnSe was synthesized by high energy ball milling technique and the details of optimizations of SnSe and Mg-doped SnSe are discussed in detail.

2 Experiment

The SnSe and Mg-doped (0.1%) SnSe were synthesised by high-energy ball milling technique at room temperature. High-purity tin pieces (Sn 99.999%, Alfa Aesar), selenium powder (Se 99.999%, Alfa Aesar), and magnesium metal turnings (Mg 99.9%, Alfa Aesar) were homogenously mixed in a tungsten carbide jar along with tungsten carbide balls. The phase and crystallinity study were examined by X-ray diffraction (XRD) PANalytical X-pert diffractometer with Cu Kα-rays (λ = 1.54 Å). The morphology of samples was evaluated by scanning electron microscope (SEM, ZEISS EVO/18).

3 Results and Discussion

The environmentally friendly and scalable, high energy ball milling process was used to synthesize pure phase of SnSe by optimising various parameters of ball milling such as RPM, milling time, on: off cycle and ball-to-powder weight ratio. After several trials, the pure phase of SnSe was observed at 300

*Corresponding authors: (E-mail: sn@ipu.ac.in)

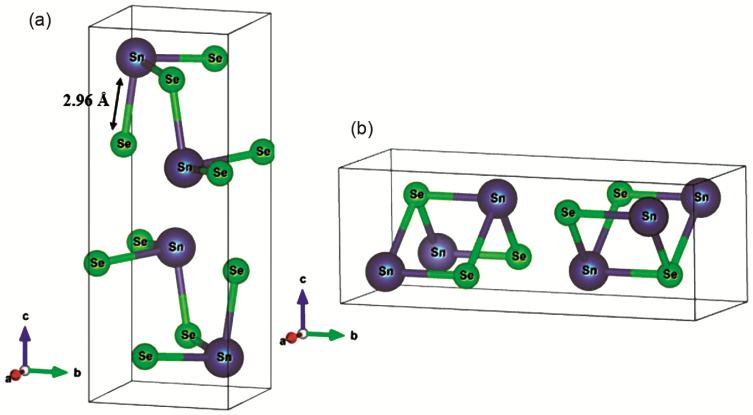

Fig. 1 — The crystal structure of (a) *Pnma* (orthorhombic) (b) *Cmcm* (monoclinic) space group of SnSe, where the atoms are connected with electrostatic attraction and van der Waals force, containing zigzag arrangement.

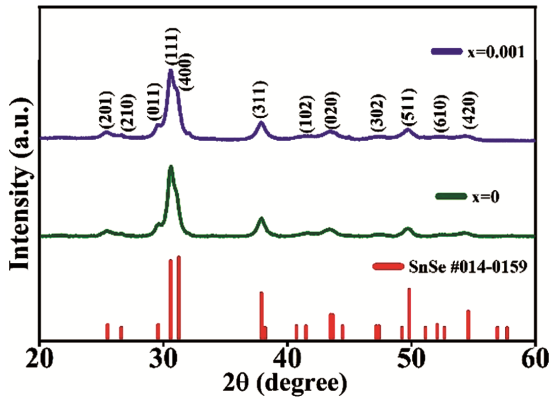

Fig. 2 — XRD pattern of purely synthesised SnSe ($Sn_{1-x}Mg_xSe$ at x=0)and 0.1% Mg-doped SnSe ($Sn_{1-x}Mg_xSe$ at x=0.001) at 300 RPM for 22 hrs, compared with SnSe standard database (JCPDS # 014-0159).

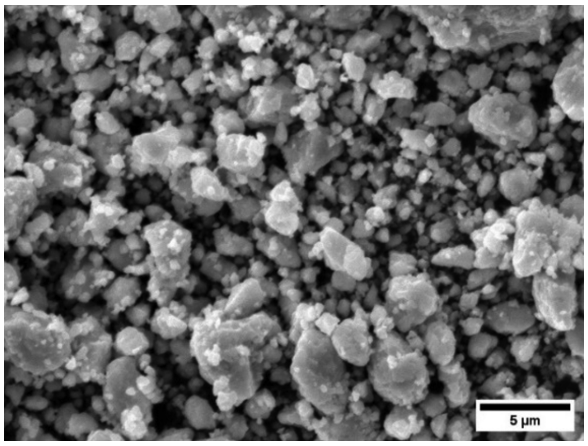

Fig. 3 — Secondary scattered SEM micrographs of SnSe samples SnSe ($Sn_{1-x}Mg_xSe$ at x=0) at 5 µm scale.

RPM and 22 hrs of milling time, which is confirmed by XRD. At this milling condition the pure phase of orthorhombic SnSe was obtained. The XRD pattern was compared with standard database (JCPDS # 014-0159) as shown in Fig. 2, and no other secondary phases were observed. After doping of 0.1% Mg at Sn site in SnSe, no structural or phase changes were observed, as seen in Fig. 2. The scanning electron microscopy (SEM) was used to analyse the morphology of purely synthesized SnSe sample ($Sn_{1-x}Mg_xSe$ at x=0), as shown in Fig. 3.

In order to determine the crystallite size of the nanostructures observed in Fig. 2, the Debye-Scherrer equation was used. The equation is given as:

$$D = \frac{k\lambda}{\beta cos\theta} \quad \ldots (1)$$

where D represents the crystallite size, k is the Scherrer constant (k = 0.9), λ denotes the wavelength of the incident X-rays (λ = 1.5418 Å), β represents the full width at half maximum (FWHM) for the diffraction peaks, and θ signifies the diffraction angle. One can clearly see the FWHM broadening which indicates the nanostructure formation.The crystallite size of pure SnSe ($Sn_{1-x}Mg_xSe$ at x=0) sample was ~9.4 nm, which decreased to ~8.3 nm with 0.1% Mg doping in SnSe ($Sn_{1-x}Mg_xSe$ at x=0.001). The broadening of FWHM for the main peak (1 1 1) was observed on Mg-doping. The lattice parameters and unit cell volume for SnSe and 0.1% Mg-doped SnSe samples were calculated from the XRD pattern. The calculated lattice parameter for SnSe are a = 11.493 Å, b = 4.168 Å, c = 4.398 Å, and unit cell volume ~210.7 Å^3. These values slightly increased to a = 11.500 Å, b = 4.147 Å, c = 4.424 Å, and unit cell volume ~ 211 Å^3 on 0.1% Mg-doping at the Sn site in SnSe. These estimated values for both the synthesized samples are in good agreement with the standard database (JCPDS # 014-0159, a= 11.496 Å, b=4.151 Å, c= 4.448 Å and unit cell volume= 212 Å^3).

The SEM image (Fig. 3) clearly exhibits the presence of different shapes and sizes and random

aggregation. The image shows the wide distribution of particle sizes, ranging from the nanometer to micrometer scale.

5 Conclusion

The orthorhombic phase of SnSe and Mg-doped SnSe were successfully synthesized by high-energy ball milling technique. From the X-ray diffraction (XRD) analysis it was found that the crystallite size was decreasing from ~9.4 nm to ~8.3 nm on 0.1% Mg-doped SnSe, with boarding of FWHM. The calculated lattice parameters and unit cell volume showed slight increase on Mg doping from a = 11.493 Å, b = 4.168 Å, c = 4.398 Å, and a unit cell volume was ~210.7 Å^3 to a = 11.500 Å, b = 4.147 Å, c = 4.424 Å, and unit cell volume was ~ 211 Å^3, which are in good agreement with standard database. The non-uniform morphology of different shape and size was observed from SEM.

Acknowledgement

The authors are grateful to Sri Sathya Sai Institute of Higher Learning Prasanthinilayam, A. P., India. SN acknowledge the FRGS (Grant No. GGSIPU/DRC/FRGS/2022/1223/13). Mukesh Kumar Bairwa acknowledge the IPRF (GGSIPU/DRC/2019/1453). Anjali Saini acknowledge the STRF (GGSIPU /DRC/2021/675).

References

1 Hyun J & Kim J, *ACS Nano*, 10 (2016) 5730.
2 Zeng L, Guo Y, Zhao F, Nie C, Li H, Shi J, Liu X, Jiang J & Zuo S, *RSC Adv*, 10 (28) (2020) 16749.
3 Kumar D K, Loskot J, Kříž J, Bennett N, Upadhyaya H M, Sadhu V, Reddy C V & Reddy K R, *Solar Energy*, 199 (2020) 570.
4 Hyun J, Park D & Kim J, *J Mater Chem A*, 6 (2018) 5627.
5 Bakhtiar Haq, AlFaify Ul S, Ahmed R, Butt F K, Laref A & Shkir M, *Phys Rev B*, 97 (2018) 075438.
6 Sajid U R, Butt F K, Tariq Z, Hayat F, Gilani R & Aleem F, *J Alloys Compd*, 695 (2017) 194.
7 Chung K M, Wamwangi D, Woda M, Wuttig M & Bensch W, *J Appl Phys*, 103 (2008) 083523.
8 Jueshuo F, Huang X, Liu F, Deng L & Chen G, *Compos Commun*, 24 (2021) 100612.
9 Ali E, *Tribol Trans*, 37 (1994) 471.
10 Abrikosov N K, *Springer*, (2013).
11 Kim S U, Duong A T, Cho S, Rhim S H & Kim J, *Surf Sci*, 651 (2016) 5.
12 Kumar M, Rani S, Singh Y, Gour K S & Singh V N, *RSC Adv*, 11 (2021) 6477.
13 Jordan R & Leoni S, *The J Phys Chem C*, 126 (2022) 14036.
14 Cheng C, Tan G, He J, Kanatzidis M G & Zhao L D, *Chem Mater*, 30 (2018) 7355.
15 Kunling P, Wu H, Yan Y, Guo L, Wang G, Lu X & Zhou X, *J Mater Chem A*, 5 (2017) 14053.
16 Chen C L, Wang H, Chen Y Y, Day T & Snyder G J, *J Mater Chem A*, 2 (2014) 11171.
17 Min J, Shi X L, Feng T, Liu W, Feng H, Pantelides S T, Jiang J, et al, *ACS Appl Mater Interf*, 11 (2019) 8051.
18 Yajie F, Xu J, Liu G Q, Tan X, Liu Z, Wang X, Shao H, Jiang H, Liang B & Jiang J, *J Electron Mater*, 46 (2017) 3182.
19 Ge Z H, Song D, Chong X, Zheng F, Jin L, Qian X, Zheng L, et al, *J Am Chem Soc*, 139 (2017) 9714.
20 Si W, Su X, Bailey T P, Hu T, Zhang Z, Tan G, Yan Y, Liu W, Uher C & Tang X, *RSC Adv*, 9 (2019) 7115.
21 Viet C N, Park H M, Shin H & Song J Y, *J Alloys Compd*, 937 (2023) 168043.
22 Kesavan M, Ho M Y, Du Y C, Chen H W & Wu H J, *Materials*, 16 (2023) 509.
23 Srikanth M, Bisht N, Saini A, Bairwa M K, Bayikadi K, Katre A & Sonnathi N, *Nanotechnology*, 33 (2022) 155710.